Wood Science and Technology (2018) 52:1229–1241
https://doi.org/10.1007/s00226-018-1026-x

ORIGINAL

Shape fixation of compressed wood by steaming: a mechanism of shape fixation by rearrangement of crystalline cellulose

Shuoye Chen[1] · Eiichi Obataya[2] · Miyuki Matsuo-Ueda[1]

Received: 19 January 2018 / Published online: 16 June 2018
© Springer-Verlag GmbH Germany, part of Springer Nature 2018

Abstract

Japanese cedar wood specimens were compressed radially using saturated water vapor at 160 °C. Their shape recovery in hot water, cellulose crystallinity, and dynamic viscoelastic properties were measured. The compressed shape of the wood was fixed completely with 120 min of steam compression. In addition, the tensile strain of the elongated steam-compressed wood specimens was recovered almost completely upon immersion in hot water. The crystallinity and crystal width of cellulose in the compressed wood increased with increasing steaming duration, corresponding to the fixation of the compressed shape and the recovery of tensile strain. These results suggested that the recrystallization or co-crystallization of cellulose, i.e., the reformation of elastic members in the wood cell walls, caused shape fixation by steam compression. When a wood specimen was compressed at 25 °C, its dynamic Young's modulus in the radial (R) direction (E_R) decreased, while its mechanical loss tangent (tan δ_R) increased remarkably. However, upon subsequent steaming, the reduced E_R began increasing and the enhanced tan δ_R began decreasing. These changes were explained by a hypothetical slip–cure model in which microfractures and slippage between or within microfibrils were cured by the rearrangement of cellulose under steaming.

✉ Eiichi Obataya
obataya.eiichi.fu@u.tsukuba.ac.jp

Shuoye Chen
chenshuoye@gmail.com

[1] Graduate School of Bioagricultural Sciences, Nagoya University, Furo-cho, Chikusa-ku, Nagoya 464-8601, Japan

[2] Graduate School of Life and Environmental Sciences, Tsukuba University, Tsukuba, Ibaraki 305-8572, Japan

Introduction

When wood is mechanically compressed in the radial (*R*) direction in an environment of high-temperature saturated steam, the compressed shape is effectively fixed, remaining unrecovered even after the specimen is rewetted and immersed in hot water. This method (referred to henceforth as steam compression) is used to densify lightweight softwood lumber to improve its material properties such as stiffness and hardness (Inoue et al. 1993; Ito et al. 1998a; Navi and Girardet 2000; Kutnar et al. 2009; Kutnar and Kamke 2012; Fang et al. 2012; Laine et al. 2013; Sandberg et al. 2013).

Although steam compression has been developed as an industrial process, the mechanism of shape fixation remains in question. Inoue et al. (1993) speculated that hydrophobization and stress relaxation of amorphous matrix polymers caused shape fixation due to steaming. However, Ito et al. (1998b) concluded that morphological changes in cellulose, rather than structural changes in the amorphous matrix polymers, induced shape fixation, because the compressed shape was not recovered when large amounts of matrix polymers were depolymerized and lost, while the crystallinity and crystal width of cellulose were significantly increased by steaming.

Hydrophobization is sometimes considered a major mechanism of steaming-induced shape fixation. Steaming causes the depolymerization of hemicelluloses, decomposition and subsequent condensation of lignin, and crystallization of cellulose (Wikberg and Maunu 2004; Inagaki et al. 2010; Yin et al. 2011; Kuribayashi et al. 2016; Guo et al. 2015, 2016, 2017; Yin et al. 2017). All of these changes reduce the hygroscopicity or equilibrium moisture content (EMC) of wood to some extent. The reduced hygroscopicity prevents the hydrothermal softening of amorphous wood polymers, and therefore, it restricts the shape recovery due to the elastic stress stored in hydrophobic cellulose fibers. In fact, acetylated wood shows less shape recovery in water, whereas it is perfectly recovered in acetone (Obataya and Yamauchi 2005). In this case, the effective shape fixation of acetylated wood is attributable to the hydrophobization, i.e., reduced accessibility to water. However, it should be noted that the steaming does not reduce the EMC of wood at high relative humidity (RH), whereas the EMC at low RH is obviously reduced by steaming (Obataya et al. 2002; Guo et al. 2015). This suggests that the reduced hygroscopicity is insufficient to explain shape fixation by steaming. If the reduced hygroscopicity did dominate the shape fixation, perfect shape fixation would be achieved when wood was steamed and then compressed. However, such pre-steaming does not perfectly fix the shape unless the wood is additionally pressed at a high temperature for a longer time (Inoue et al. 2008). Thus, the importance of the reduced hygroscopicity in shape fixation by steaming remains in question.

From the considerations above, the morphological changes in cellulose and cross-linking in lignin are considered as the most reasonable mechanisms underlying shape fixation by steaming. In this study, the shape recovery of steam-compressed wood from both compressive strain and reversed tensile strain after

elongation was observed to prove the reformation of elastic members in the steam-compressed wood cell walls. X-ray diffractometry (XRD) and vibration measurements were performed on the steam-compressed wood to understand the damage to the wood cell walls under compression and the "curing" thereof by steaming.

Materials and methods

Compression of wood in steam

Figure 1 shows the shape of the tested wood specimens. Japanese cedar wood (*Cryptomeria japonica* D. Don) was cut into blocks with dimensions of 29 (longitudinal, *L*) × 29 (tangential, *T*) × 29 mm^3 (radial, *R*). The average material density in dry conditions was 376 kg/m^3 (360–395 kg/m^3). These specimens were soaked in water at 25 °C for 1 week, and the water-swollen specimens, measuring 31 mm in the *R* direction, were compressed in the *R* direction in an autoclave at 160 °C for 15, 30, 60, 90, 120, 240, and 480 min, as described in a previous study (Obataya and Chen 2018). The compressive strain was 52% in wet conditions. After the steam compression, water was drained from the autoclave and the autoclave was immediately cooled to 100 °C. The specimens, remaining compressed, were dried in the autoclave at 100 °C for 12–18 h; afterward, the wood specimens were completely dried in an oven at 105 °C and their dry masses and dimensions were measured. Twelve specimens were used for each treatment condition.

Half of the steam-compressed blocks (Fig. 1b) were subjected to the following recovery tests. The other specimens were stacked and adhered with epoxy glue into rods, which were sliced into strips as shown in Fig. 1c. The strips were used for the vibration testing described in the section "Vibration testing".

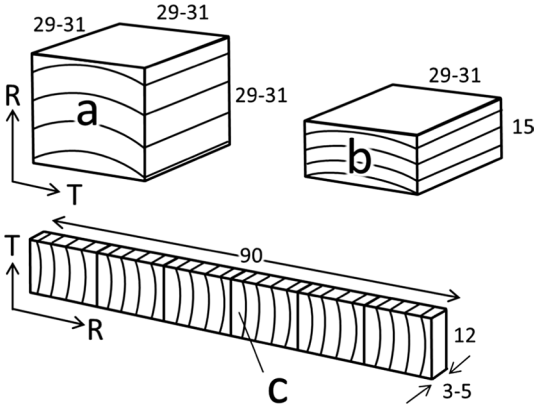

Fig. 1 Shape of wood specimens tested. **a** Uncompressed block, **b** compressed block, **c** glued strips. All measurements in millimeters

Recovery of compressive strain

The compressed wooden blocks (Fig. 1b) were soaked in water at 25 °C for 1 week and then boiled in water at 95 °C for 1 h. After the recovery treatment, the specimens were air-dried at 25 °C and 60% RH for 7–10 days, followed by oven-drying at 105 °C for 1 day, to determine their recovered dimensions in absolutely dry conditions. Figure 2 illustrates the changes in the shapes of the wood specimens by steam compression and recovery treatment. The recovery of compressive strain (SR_C) was evaluated by the following equation:

$$SR_C \equiv \frac{t_{CR} - t_C}{t_{C0} - t_C} \tag{1}$$

where t_{C0}, t_C, and t_{CR} are the thickness of the uncompressed, steam-compressed, and recovered specimens in the *R* direction, respectively.

Tensile setting and recovery

If the major mechanism of shape fixation is the stress relaxation of wood polymers or reduced hygroscopicity, the reversed tensile deformation of compressed wood is expected to remain unrecovered upon immersion in hot water. To verify this prediction, untreated and steam-compressed wood specimens were elongated in the *R* direction, and the remaining tensile strain was observed before and after immersion in hot 95 °C water.

First, wooden blocks were compressed in steam as described in the section "Compression of wood in steam". The steam-compressed wooden blocks were then immersed in 95 °C water to recover their shape. Next, the recovered blocks were stacked and glued with epoxy resin. The glued specimens were sliced into strips, as exhibited in Fig. 1c.

Figure 3 illustrates the changes in the lengths of a given strip by the following tensile setting and recovery. The strips were oven-dried at 105 °C for 1 day and measured in length. The strips were then soaked in water for 12 h, and the wetted strips were dried in ambient conditions (21–23 °C and 50–60% RH) under constant tensile stress (0.2 MPa) applied in the *R* direction. This tension induced large (10–23%) tensile strain by the mechano-sorptive effect, and the extended length was

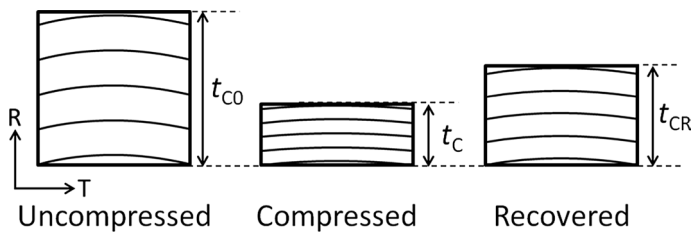

Fig. 2 Changes in the cross section of wood by steam compression and recovery treatment

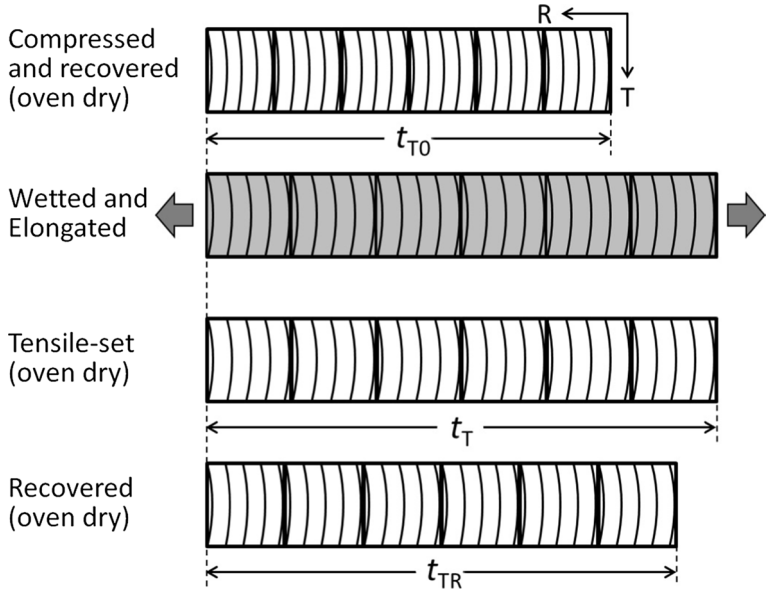

Fig. 3 Changes in the length of glued strips by tensile setting and recovery treatment

temporarily set during drying. Hereafter, it is referred to this process as tensile setting and the processed specimens are described as tensile-set. The tensile-set strips were dried at 105 °C for 1 day to determine their oven-dried lengths and then soaked in water for 1 week followed by immersion in water at 95 °C and atmospheric pressure for 1 h to recover the tensile strain temporarily set during drying. The strips were finally oven-dried to determine their recovered lengths in dry conditions. The recovery of tensile strain (SR_T) was evaluated by the following equation:

$$SR_T \equiv \frac{t_T - t_{TR}}{t_T - t_{T0}} \tag{2}$$

where t_{T0}, t_T, and t_{TR} are the thicknesses of steam-compressed, elongated, and recovered specimens in the R direction, respectively. Both SR_C and SR_T are defined as 1 for complete recovery, and 0 for complete fixation.

Vibration testing

The free–free flexural vibration method (Obataya et al. 2000) was used to measure the dynamic Young's modulus (E_R) and mechanical loss tangent (tan δ_R) of the steam-compressed wood along the R direction. The wooden strips shown in Fig. 1c were conditioned at 25 °C and 60% RH, and their E_R values were calculated from the resonance frequencies of the first vibration mode, while the tan δ_R values were calculated from the half-width of the resonance curves.

XRD measurement

The steam-compressed wood was ground using a mill and sieved using a stainless steel sieve (0.350-mm openings, or 42-mesh). Pellets of 0.5 mm in thickness and 7 mm in diameter were formed from 0.05 g of the sieved powder by pressing in a mold under 10 kN. Five pellets were formed for each treatment condition. For XRD measurement, an X-ray diffractometer (Ultima IV, Rigaku Co., Japan) was used: The incident X-ray radiation was the Cu Kα characteristic X-ray passing through a nickel filter with a power of 40 kV and 40 mA. The reflection intensity was recorded through the scanning angle (2θ) range from 5° to 45° at a scanning speed of 2.5°/min. The crystallinity index (CI) was calculated by the Segal method (Segal et al. 1959) and the following equation:

$$\mathrm{CI} = \frac{I_{200} - I_{\mathrm{Am}}}{I_{200}} \times 100(\%) \tag{3}$$

where I_{200} is the maximum reflection intensity of the cellulose (200) peak, and I_{Am} is the minimum reflection intensity near the 2θ angle of 18.5°.

The crystal width is defined as the average thickness of cellulose crystallites perpendicular to the cellulose (200) plane (D_{200}). Based on the Scherrer equation (Alexander 1969), D_{200} was calculated by the following equation:

$$D_{200} = \frac{K\lambda}{B \cdot \cos\theta_{200}} \tag{4}$$

where K is the Scherrer constant (0.9), λ the incident X-ray wavelength (0.1542 nm), B the half bandwidth (full width at half maximum, FWHM) of the (200) peak in radians, and θ_{200} is the Bragg angle for the (200) plane.

Results and discussion

Loss in mass by steaming

Figure 4 shows the effects of steaming duration on the loss in mass by steam compression and subsequent soaking in hot water. The slight mass loss of the unheated wood is attributed to the loss of water-soluble extractives. The mass loss increases as the steaming duration is increased, predominantly because of the hydrolysis of hemicelluloses. However, it reaches 15% at most in the present case, suggesting that at least half of the hemicelluloses remain in the wood cell wall.

Strain recovery and possible mechanism of shape fixation

The recovery of compressive strain ($\mathrm{SR_C}$) is plotted against the steaming duration in Fig. 5. The $\mathrm{SR_C}$ value decreases as the steaming duration is increased to 120 min; for further increases in duration, the compressed shape is perfectly fixed ($\mathrm{SR_C} = 0$).

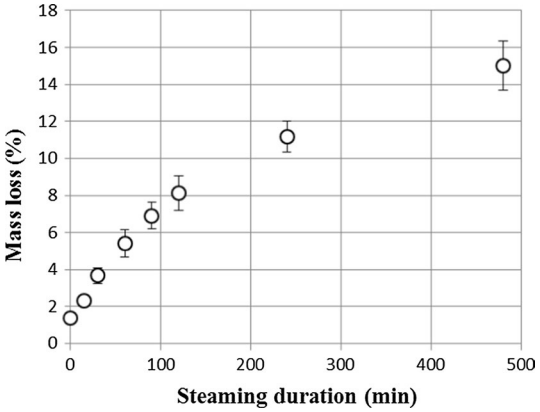

Fig. 4 Loss in mass by steam compression and subsequent recovery treatment as a function of steaming duration. Bars: standard deviations

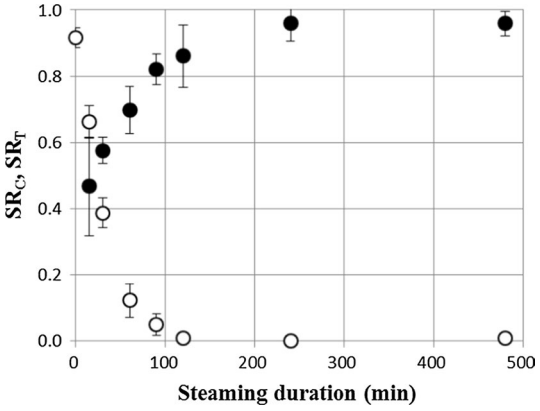

Fig. 5 Recovery of compressive strain (SR_C) and that of tensile-set (SR_T) by immersion in hot water as a function of steaming duration. Open circles: recovery of compressive strain (SR_C); filled circles: recovery of tensile strain (SR_T); bars: standard deviations

Inoue et al. (1993, 2008) speculated that the stress relaxation and hydrophobization of wood from the depolymerization of amorphous cell-wall polymers caused the shape fixation of wood under steaming. If this was true, the reversed (tensile) deformation of steam-compressed wood would remain unrecovered after immersion in hot water. In Fig. 5, the recovery of tensile setting (SR_T) is plotted against the steaming duration. The SR_T value increases as the steaming duration is increased. After 120 min of steaming, the tensile deformation of the elongated steam-compressed wood is almost completely recovered by immersion in hot water. Therefore, stress relaxation and hydrophobization of amorphous wood polymers are insufficient to explain shape fixation induced by steam compression.

To explain the recovery of tensile-set wood, it must be assumed the formation of a new elastic element in the compressed wood. Figure 6 illustrates an elasto-plastic model of the proposed recovery mechanism of tensile-set wood. In a steam-compressed wood specimen (Fig. 6a), compressive strain is retained temporarily by the plastic deformation of the amorphous matrix polymers, while elastic energy is stored in the hydrophobic and elastic fibers in the cell walls.

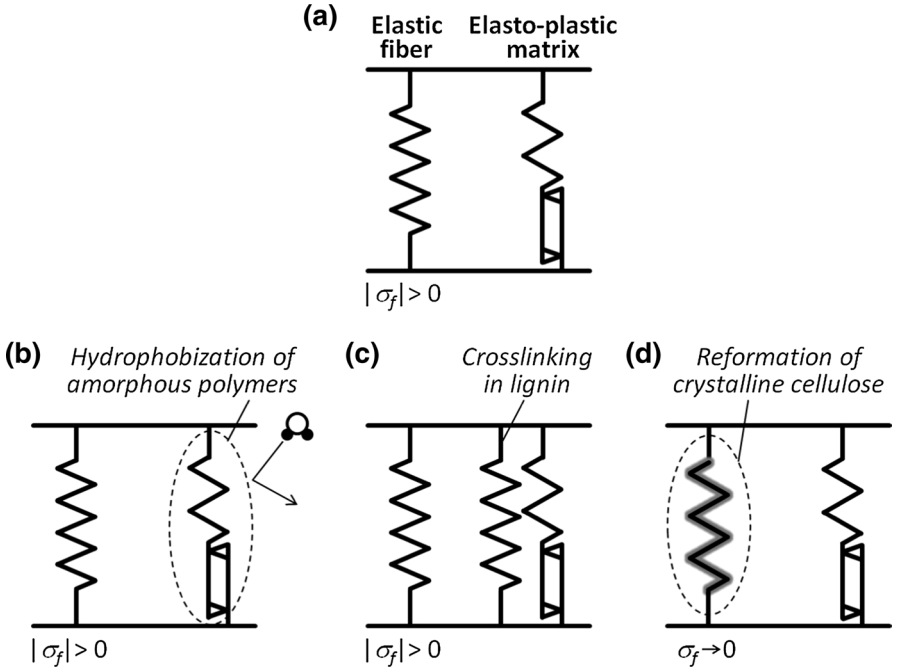

Fig. 6 An elasto-plastic model of (**a**) compressed and (**b**–**d**) steam-compressed wood to explain the recovery of tensile-set wood

Figure 6b–d exhibits possible mechanisms for the formation of a new elastic element allowing the recovery of the tensile-set wood. The first mechanism (Fig. 6b) is hydrophobization, sometimes considered a major mechanism of shape fixation. It prevents the moisture sorption of the amorphous matrix polymers and subsequent hygrothermal softening. However, the EMC of wood at 25 °C and 60% RH is reduced by only 2% (from 11 to 9%) in the present case. In addition, reduced hygroscopicity does not explain imperfect shape fixation by pre-steaming (Inoue et al. 2008) or the recovery of tensile strain (Fig. 5). Therefore, hydrophobization seems a minor mechanism of shape fixation due to steaming.

The second mechanism (Fig. 6c) is the formation of cross-links, which can mechanically restrict the shape recovery of polymeric materials. It has been suggested that cross-linking treatments, such as formalization, allow effective shape fixation (Inoue et al. 1994). Cross-linking reactions also occur in lignin by dry heating (Tjeerdsma et al. 1998) as well as by steaming (Wikberg and Maunu 2004; Yin et al. 2017). If the cross-linking was tight and dense enough to mechanically fix the compressed shape of wood, swelling of the wood would be effectively restricted. However, the wet volume of wood is not always reduced by steaming, whereas it is effectively reduced by oven heating (Obataya et al. 2002; Obataya and Higashihara 2017). Therefore, the mechanical contribution of cross-linking is questionable as a major mechanism of shape fixation.

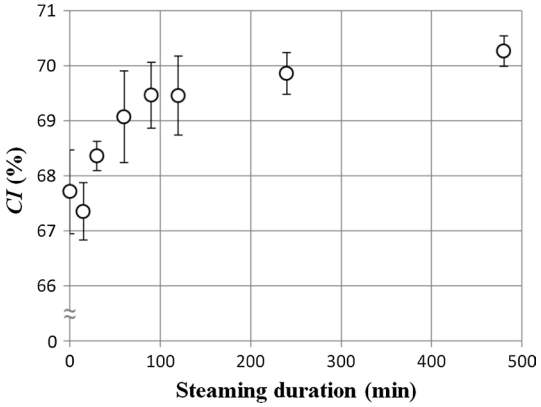

Fig. 7 Crystallinity index (CI) of steam-compressed wood as a function of steaming duration. Bars: standard deviations

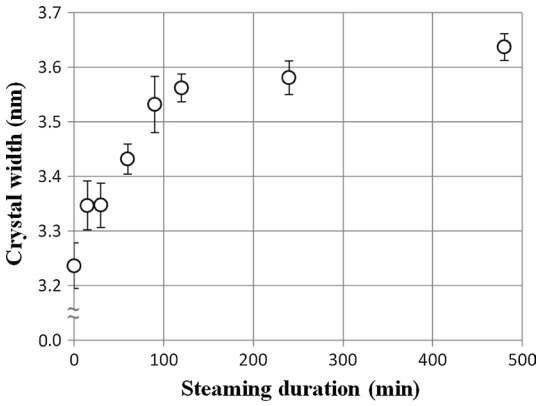

Fig. 8 Crystal width of steam-compressed wood as a function of steaming duration. Bars: standard deviations

The third mechanism (Fig. 6d), the reformation of elastic fibers, is the most reasonable explanation for the recovery of tensile-set wood and the fixation of compressive strain. Although crystalline cellulose is inaccessible to water and thermally stable in dry conditions, it can be slightly rearranged by high-temperature steaming. The crystallinity of cellulose is known to increase under steaming (Dwianto et al. 1996; Ito et al. 1998b; Bhuiyan et al. 2000; Andersson et al. 2005; Guo et al. 2016; Yin et al. 2017), and some models have been proposed to explain the rearrangement in cellulosic microfibrils during this crystallization (Inagaki et al. 2010; Kuribayashi et al. 2016; Guo et al. 2016).

Figures 7 and 8 show the crystallinity index (CI) and the crystal width of steam-compressed wood as functions of steaming duration. Both the CI and crystal width increase with steaming, corresponding to the decrease in SR_C and increase in SR_T shown in Fig. 5. This result coincides with earlier investigations (Ito et al. 1998b; Bhuiyan et al. 2000; Andersson et al. 2005; Guo et al. 2016; Yin et al. 2017) and implies that the changes in cellulose crystallinity are tightly connected to the shape fixation by steam compression.

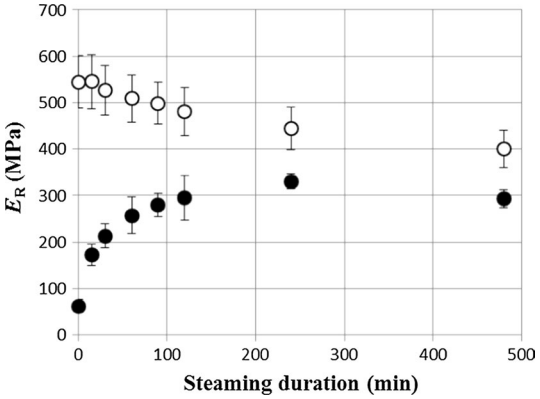

Fig. 9 Changes in dynamic Young's modulus (E_R) of wood in *R* direction plotted against steaming duration. Open circles: uncompressed and steamed; filled circles: steamed under compression; bars: standard deviations

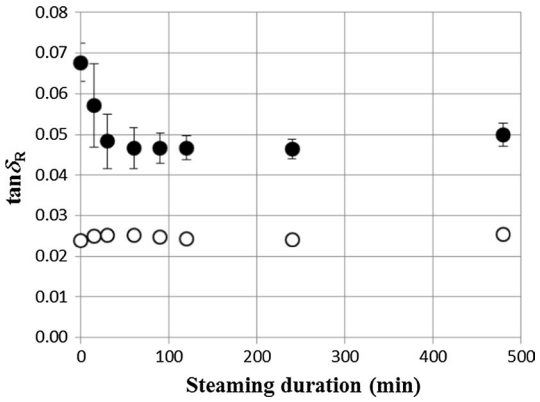

Fig. 10 Changes in mechanical loss tangent (tan δ_R) of wood in *R* direction plotted against steaming duration. Open circles: uncompressed and steamed; filled circles: steamed under compression; bars: standard deviations

When wood is compressed, stress is stored in elastic spring structures, mainly comprising cellulosic microfibrils. The stored stress remains unless the crystalline cellulose is seriously depolymerized, as in the case of oven heating, and drives the shape recovery of wood. However, the stored stress disappears with the reformation of spring structures, and these reformed springs allow the fixation of the compressed shape (decreased SR_C) as well as the recovery of tensile setting (increased SR_T).

Changes in dynamic viscoelastic properties

Figures 9 and 10 show the changes in E_R and tan δ_R of the wood steam-compressed in the *R* direction. With compression, E_R decreases and tan δ_R increases considerably. Wood becomes softer and more ductile in the *R* direction under radial compression (Hirano et al. 2016), whereas it becomes stiffer and stronger in the longitudinal direction. The reduction in E_R is explained by the reduced flexural rigidity of the buckled cell walls, as well as changes in the angle of the cell walls: radial cell walls do not effectively support the axial stress in the *R* direction after buckling

or falling sideways under compression. Meanwhile, the drastic threefold increase in tan δ_R can be attributed to the increased internal friction of the wood cell wall due to microfracturing, rather than to the changes in cell shape, because tan δ is a shape-independent parameter.

Under steaming, the reduced E_R increases and the enhanced tan δ_R decreases; these trends correspond well to the changes in strain recovery (Fig. 5) and the recrystallization of cellulose (Figs. 7, 8). This implies that the mechanical properties of the wood steam-compressed in the *R* direction are closely connected to the shape fixation and structural changes in the crystalline cellulose.

In Figs. 9 and 10, the effects of steaming (without compression) on the E_R and tan δ_R values of uncompressed wood are also exhibited. The E_R value of uncompressed wood decreases monotonically as the steaming duration is increased, while the tan δ_R value remains almost unchanged. E_R is probably decreased by the decomposition of hemicelluloses, which are important in connecting the fibers and matrix polymers to rigidify the wood cell walls. In addition, the depolymerization of the amorphous matrix polymers (enhancing tan δ_R), crystallization of cellulose, and cross-linking in lignin (reducing tan δ_R) presumably compensate for each other, leading to a relatively stable tan δ_R value.

To explain all the results above, here it is proposed that the microfractures induced by compression are cured by the subsequent steaming. This hypothesis is illustrated in Fig. 11. When wood is compressed, the cell walls are tightly buckled and folded. Although serious delamination and rupture are not observed in the cross section of the compressed wood specimen under optical microscopy, some degree of microfracture, i.e., slippage between and/or within the microfibrils occurs in the wood cell walls. The drastic increase in tan δ_R (Fig. 10) due to compression without steaming cannot be explained without assuming the microfracture of the cell wall.

Because the elastic energy stored in the microfibrils remains unrelaxed by the microfracture, the compressed shape is recovered by the softening and swelling of the amorphous matrix polymers. However, the microfracture within and/or between

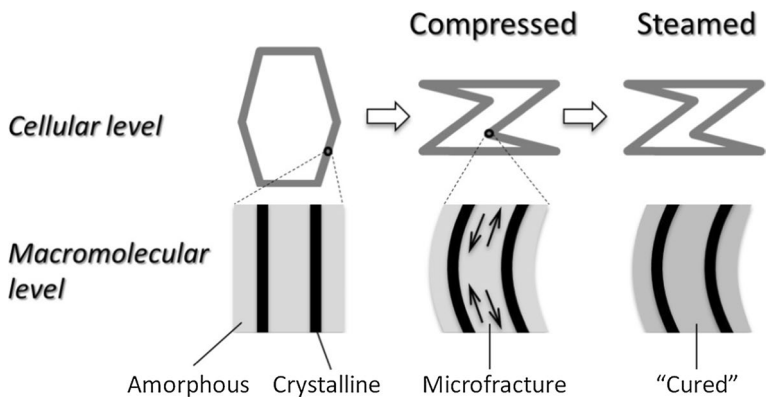

Fig. 11 A slip–cure model to explain shape fixation and changes in mechanical properties of wood under steam compression

microfibrils is cured by steaming, which allows the rearrangement of cellulose (Inagaki et al. 2010; Kuribayashi et al. 2016; Guo et al. 2016). In this curing process, the elastic energy stored in the microfibrils is relaxed and the shape of wood is perfectly fixed by the reassembled fibers. At the same time, the decreased E_R begins to increase, and the increased tan δ_R begins to decrease by the reassembling of the fractured fibers.

This model does not contradict the slighter influence of steaming on the E_R and tan δ_R of uncompressed wood. Because uncompressed wood experiences no mechanical damage or changes in the alignments of the cell walls, the mechanical properties of the uncompressed wood are only influenced by the depolymerization of hemicelluloses, cross-linking of lignin, and crystallization of cellulose during steaming.

The shape fixation is not achieved by a single mechanism, because steam compression induces multiple mechanical and chemical changes in the wood cell wall. However, the present slip–cure concept is considered the most reasonable, because it explains the shape recovery, shape fixation, and drastic changes in the mechanical properties of compressed wood with the least contradiction.

Conclusion

The compressed shape of wood was fixed by steaming at 160 °C for 120 min. Meanwhile, the tensile strain of elongated steam-compressed wood was recovered almost completely by immersion in hot water. Because these changes corresponded well to the changes in crystallinity and crystal width of cellulose, the structural changes in crystalline cellulose were proposed as the major mechanism underlying shape fixation by steaming. To explain the changes in mechanical properties of wood compressed by steaming, a slip–cure model was proposed: (1) the wood cell wall is tightly folded by compression, and microfracture between and/or within the microfibrils reduces E_R and enhances tan δ_R; (2) the slipped microfibrils are reformed by the steaming-induced rearrangement of crystalline cellulose, consequently fixing the compressed shape, increasing the reduced E_R, and decreasing the enhanced tan δ_R.

References

Alexander LE (1969) X-ray diffraction methods in polymer science. Wiley, Amsterdam, pp 423–424

Andersson S, Serimaa R, Väänänen T, Paakkari T, Jämsä S, Viitaniemi P (2005) X-ray scattering studies of thermally modified Scots pine (*Pinus sylvestris* L.). Holzforsch 59:422–427

Bhuiyan MTR, Hirai N, Sobue N (2000) Changes of crystallinity in wood cellulose by heat treatment under dried and moist conditions. J Wood Sci 46:431–436

Dwianto W, Tanaka F, Inoue M, Norimoto M (1996) Crystallinity changes of wood by heat or steam treatment. Bull Wood Res Inst Kyoto Univ 83:47–49

Fang CH, Mariotti N, Cloutier A, Koubaa A, Blanchet P (2012) Densification of wood veneers by compression combined with heat and steam. Eur J Wood Prod 70:155–163

Guo J, Songa K, Salmén L, Yin Y (2015) Changes of wood cell walls in response to hygro-mechanical steam treatment. Carbohydr Polym 115:207–214

Guo J, Rennhofer H, Yin Y, Lichtenegger HC (2016) The influence of thermo-hygro-mechanical treatment on the micro- and nanoscale architecture of wood cell walls using small- and wide-angle X-ray scattering. Cellulose 23:2325–2340

Guo J, Yin J, Zhang Y, Salmén L, Yin Y (2017) Effects of thermo-hygro-mechanical (THM) treatment on the viscoelasticity of in situ lignin. Holzforschung 71(6):455–460
Hirano A, Obataya E, Adachi K (2016) Potential of moderately compressed wood as an elastic component of wooden composites. Eur J Wood Prod 74:685–691
Inagaki T, Siesler HW, Mitsui K, Tsuchikawa S (2010) Difference of the crystal structure of cellulose in wood after hydrothermal and aging degradation: a NIR spectroscopy and XRD study. Biomacromolecules 11:2300–2305
Inoue M, Norimoto M, Tanahashi M, Rowell RM (1993) Steam or heat fixation of compressed wood. Wood Fib Sci 25:224–235
Inoue M, Minato K, Norimoto M (1994) Permanent fixation of compressive deformation of wood by crosslinking. Mokuzai Gakkaishi 40:931–936
Inoue M, Sekino N, Morooka T, Rowell RM, Norimoto M (2008) Fixation of compressive deformation in wood by pre-steaming. J Trop For Sci 20(4):273–281
Ito Y, Tanahashi M, Shigematsu M, Shinoda Y, Otha C (1998a) Compressive-molding of wood by high-pressure steam-treatment: part 1. Development of compressively molded squares from thinnings. Holzforsch 52:211–216
Ito Y, Tanahashi M, Shigemitsu M, Shinoda Y (1998b) Compressive-molding of wood by high-pressure steam treatment: part 2. Mechanism of permanent fixation. Holzforschung 52:217–221
Kuribayashi T, Ogawa Y, Rochas C, Matsumoto Y, Heux L, Nishiyama Y (2016) Hydrothermal transformation of wood cellulose crystals into pseudo-orthorhombic structure by cocrystallization. ACS Macro Lett 5:730–734
Kutnar A, Kamke FA (2012) Influence of temperature and steam environment on set recovery of compressive deformation of wood. Wood Sci Technol 46:953–964
Kutnar A, Kamke FA, Sernek M (2009) Density profile and morphology of viscoelastic thermal compressed wood. Wood Sci Technol 43:57–68
Laine K, Rautkari L, Hughes M (2013) The effect of process parameters on the hardness of surface densified Scots pine solid wood. Eur J Wood Prod 71:13–16
Navi P, Girardet F (2000) Effects of thermos-hydro-mechanical treatment on the structure and properties of wood. Holzforschung 54:287–293
Obataya E, Chen S (2018) Shape recovery and anomalous swelling of steam-compressed wood by swimming ring-like expansion of cell lumina. Wood Sci Technol. https://doi.org/10.1007/s00226-018-1018-x
Obataya E, Higashihara T (2017) Reversible and irreversible dimensional changes of heat-treated wood during alternate wetting and drying. Wood Sci Technol 51:739–749
Obataya E, Yamauchi H (2005) Compression behaviors of acetylated wood in organic liquids Part II. Drying–set and its recovery. Wood Sci Technol 39(7):546–559
Obataya E, Ono T, Norimoto M (2000) Vibrational properties of wood along the grain. J Mater Sci 35:2993–3001
Obataya E, Higashihara T, Tomita B (2002) Hygroscopicity of heat-treated wood III. Effect of steaming on the hygroscopicity of wood. Mokuzai Gakkaishi 48:348–355
Sandberg D, Haller P, Navi P (2013) Thermo-hydro and thermo-hydro-mechanical wood processing: an opportunity for future environmentally friendly wood products. Wood Mater Sci Eng 8:64–88
Segal L, Creely JJ, Martin AE, Conrad CM (1959) An empirical method for estimating the degree of crystallinity of native cellulose using the X-ray diffractometer. Text Res J 29:786–794
Tjeerdsma BF, Boonstra M, Pizzi A, Takely P, Militz H (1998) Characterization of thermally modified wood: molecular reasons for wood performance improvement. Holz Roh Werkst 56:149–153
Wikberg H, Maunu SL (2004) Characterisation of thermally modified hard- and softwoods by ^{13}C CPMAS NMR. Carbohydr Polym 58:461–466
Yin Y, Berglund L, Salmén L (2011) Effect of steam treatment on the properties of wood cell walls. Biomacromol 12:194–202
Yin J, Yuan T, Lu Y, Song K, Li H, Zhao G, Yin Y (2017) Effect of compression combined with steam treatment on the porosity, chemical composition and cellulose crystalline structure of wood cell walls. Carbohydr Polym 155:163–172

Publisher's Note Springer Nature remains neutral with regard to jurisdictional claims in published maps and institutional affiliations.